[16]A. J. Epstein, E. M. Conwell, and J. S. Miller, to be published; E. M. Conwell, Phys. Rev. B 19, 2409 (1979).
[17]A. Von Middendorff, Cryogenics 11, 318 (1971).
[18]J. A. Woolam, Rev. Sci. Instrum. 41, 284 (1970).
[19]F. J. Blatt, A. D. Caplin, C. K. Chiang, and P. A. Schroeder, Solid State Commun. 15, 411 (1974).
[20]I. F. Schegolev, Phys. Status Solidi (a) 12, 9 (1972).

Fermi Surface of Incommensurate Mercury-Chain Compounds

F. S. Razavi and W. R. Datars
Department of Physics, McMaster University, Hamilton, Ontario L8S 4M1, Canada

and

D. Chartier and R. J. Gillespie
Department of Chemistry, McMaster University, Hamilton, Ontario L8S 4M1, Canada

(Received 15 January 1979)

Measurement of the de Haas–van Alphen effect at 1.1 K in the linear-chain mercury compound $Hg_{3-\delta}AsF_6$ shows that the Fermi surface consists of a set of straight or nearly straight cylinders with axes along the $\vec{c}$ direction. The cylinders are formed from one-dimensional Fermi-surface sheets by the interaction of mutually perpendicular mercury chains and by translation by superlattice vectors resulting from the periodicity of the incommensurate mercury chains.

The linear-chain mercury compounds, $Hg_{3-\delta}AsF_6$ and $Hg_{3-\delta}SbF_6$, exhibit anisotropic electrical[1,2] and optical[3,4] properties. These compounds contain infinite, nonintersecting chains of mercury atoms running along $\vec{a}$ and $\vec{b}$ directions of the tetragonal structure.[5] The separation between mercury atoms is incommensurate with the tetragonal host lattice. Direct measurements of the Fermi surface of these compounds would be highly desirable to determine the Fermi surface of one-dimensional, nonintersecting conducting chains. We report the results of a de Haas–van Alphen (dHvA) experiment on $Hg_{3-\delta}AsF_6$ which explain the anisotropic electrical conduction and support a model of the Fermi surface formed from one-dimensional bands.

The dHvA effect was observed at 1.1 K in a magnetic field range 3–5.5 T with the low-frequency modulation technique.[6] Single-crystal samples of $Hg_{3-\delta}AsF_6$ with dimensions $2\times2\times1$ mm^3 contained in a sealed sample holder were mounted in a sensitive modulation-pickup–coil assembly. Measurements were made for magnetic field directions between the $\vec{c}$ axis and the (001) plane which were determined optically. Directions in the isotropic (001) plane could not be determined optically so that it was not known where the plane that was studied intersected the (001) plane. The data were collected on magnetic tape and analyzed by computer.

dHvA frequencies of $Hg_{3-\delta}AsF_6$ shown in Fig. 1 consist of six branches with minima along the $\vec{c}$ axis. Five branches, α, β, δ, and ϵ, extend 64 $\pm$ 10° from the $\vec{c}$ axis toward the (001) plane. Branch μ is over a smaller angular range of $\pm$ 20° from the $\vec{c}$ axis and is not observed below a magnetic field of 4.6 T. Table I shows the values of the dHvA frequencies and corresponding cross-sectional areas of the Fermi surface measured with the magnetic field along the $\vec{c}$ axis. A low frequency with a value of approximately 48 T, which is not shown in Table I and Fig. 1, was observed over a very small angular range about the $\vec{c}$ axis. No dHvA frequencies were found in a careful search with magnetic-field directions in the (001) plane, indicating that no closed Fermi-surface pieces exist.

Cyclotron masses were determined from the temperature dependence of the dHvA amplitude in a crystal where the magnetic field was oriented 20° from the $\vec{c}$ axis. The cyclotron masses of the branches with sufficient amplitude for the mass determination (the γ, δ, and ϵ branches) are the same to within experimental error and have a value of $(0.35\pm0.05)m_0$.

The angular dependence of the dHvA frequencies suggests pieces of Fermi surface which are cylinders along the $\vec{c}$ axis in k space. The cross-sectional area of a straight cylinder varies as $A_0\sec\theta$, where A_0 is the cross-sectional area perpendicular to the axis of the cylinder and θ is the angle between the magnetic field direction and the cylinder axis. The dHvA frequencies in Fig. 1 follow this $\sec\theta$ dependence closely for values of

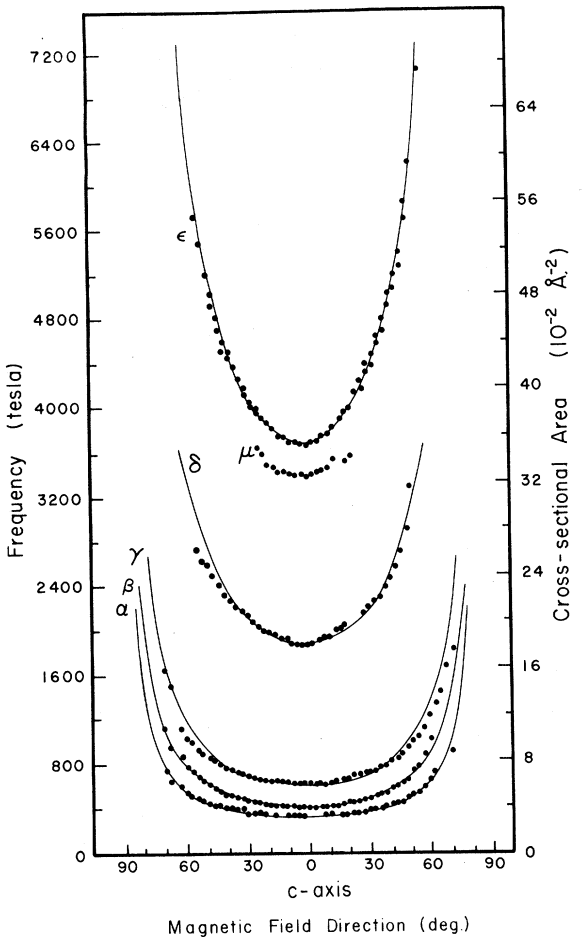

FIG. 1. dHvA frequencies and extremal cross-sectional area of the Fermi surface of $Hg_{3-\delta}AsF_6$ for magnetic-field directions in a plane containing the $\vec{c}$ axis and perpendicular to the (001) plane. The solid lines are the fit to a set of straight, Fermi-surface cylinders with axes parallel to $\vec{c}$.

A_0 and corresponding frequencies, F_0, given in Table I, indicating that the Fermi surface of $Hg_{3-\delta}AsF_6$ consists of a set of straight or nearly straight cylinders. The secθ behavior is independent of the shape of area A_0, so that no information about the shape of the cross section A_0 is obtained from the fit in Fig. 1.

The Fermi surface of $Hg_{3-\delta}AsF_6$ is constructed by first filling one-dimensional electron k states of each mercury chain.[7] The total number of electrons from the mercury chain [(two valence electrons per Hg atom)×(2.79 Hg atoms in each chain in a unit cell at[8] 10 K)×(four chains per unit cell)] is 22.32 electrons. Four of these electrons go to AsF_6^{-1} ions. The remaining 18.32 electrons occupy 9.16 states/spin. Thus, the states of the

TABLE I. dHvA frequencies and extremal cross-sectional areas of $Hg_{3-\delta}AsF_6$ with the magnetic field along the $\vec{c}$ axis for a cylindrical fit to experimental data and for our model calculation.

	Experimental		Calculated	
Orbit	A_0 (A^{-2})	F_0 (T)	A_0 (A^{-2})	E_0 (T)
α	0.0325	340	0.032	331
β	0.0395	413	...	...
γ	0.0598	626	0.060	627
δ	0.178	1860	0.18	1870
μ	0.326	3413	0.33	3420
ϵ	0.352	3680	0.36	3750

four $\vec{a}$ and $\vec{b}$ chains are filled up to $2.29\pi/a_L$, where a_L is a tetragonal lattice vector. The first and second zones are filled and the Fermi surfaces are sheets defined by $k_a = \pm 0.29\pi/a_L$ and $k_b = \pm 0.29\pi/a_L$ in the third zone. The energy band for each surface is at least twofold degenerate because of the two parallel chains in the $\vec{a}$ and $\vec{b}$ directions in a unit cell. Projection of the Fermi-surface sheets on the (001) plane is shown in Fig. 2(a).

There is no finite area between the one-dimensional Fermi-surface sheets parallel to the $\vec{a}$ or $\vec{b}$ directions. However, with even a small overlap of the $\vec{a}$ and $\vec{b}$ chains, interaction couples the bands where the Fermi-surface sheets cross. This produces electronlike square cylinders with axes parallel to $\vec{c}$ giving the electron orbit γ shown in Fig. 2(a). A holelike square cylinder is formed between the sheets giving the hole orbit ϵ. The calculated cross-sectional areas and the corresponding frequencies of the electron and hole cylinders for the magnetic field parallel to $\vec{c}$ agree exactly with those found for the γ and ϵ branches, respectively, as shown in Table I, and are assigned to them.

Now, it is necessary to introduce the periodicity of the Hg-Hg intrachain spacing $a_{Hg} = 2.67$ Å which is incommensurate with the tetragonal lattice vector $a_L = 7.442$ Å. In reciprocal-lattice space, the difference between the intrachain reciprocal-lattice vector and the vector spanning three unit cells of the reciprocal tetragonal lattice vector is $\delta^* = 0.179$ Å^{-1}. This incommensurability exists along the $\vec{a}$ and $\vec{b}$ directions. Thus, we expect that the reciprocal-lattice points in the tetragonal unit cell can be translated along the resultant of δ^* along $\vec{a}$ and $\vec{b}$. The resultant is $2^{1/2}\delta^*$ along $\langle 110 \rangle$ directions and results in a su-

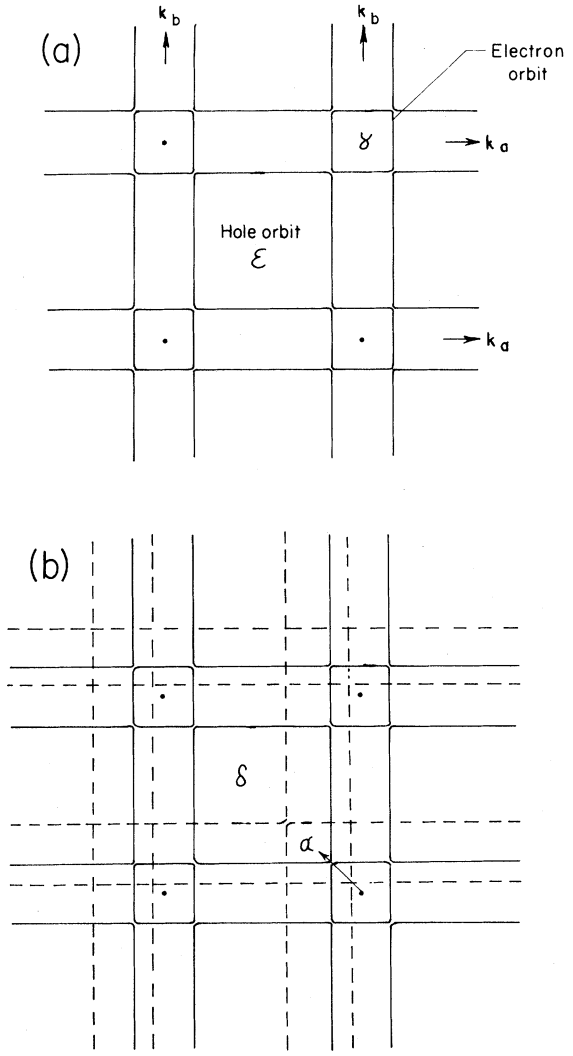

FIG. 2. Fermi surface of $Hg_{3-\delta}AsF_6$ constructed from one-dimensional bands. (a) The Intersection of one-dimensional Fermi-surface sheets parallel to k_a and k_b directions. The center of the γ orbit is the Γ center of the zone. (b) The translation, shown as dashed lines, of the intersecting one-dimensional bands by one superlattice vector $2^{1/2}\delta^*$.

perlattice translation. This translation vector is consistent with the reciprocal-lattice vectors of the monoclinic structure[8] of the linear chains below 120 K. The shortest reciprocal-lattice vector is $(\delta,\delta,0)$ away from a reciprocal-lattice vector of the body-centered tetragonal structure. The presence of a superlattice in metals[9] and compounds[10] has the effect of adding additional Brillouin-zone boundaries and energy gaps in the band structure.[11,12]

The result of translation of Fig. 2(a) by one superlattice vector $2^{1/2}\delta^*$ is shown in Fig. 2(b). This first-order translation generates a holelike orbit δ, an electronlike orbit α, and a small electronlike orbit with a frequency of 45 T at the small overlap of the γ squares. The cross-sectional areas and dHvA frequencies of the α and δ orbits produced by the first-order translation with no adjustable parameters are in excellent agreement with the experimental results shown in Table I. The electronlike orbit with a predicted frequency of 45 T is detected as an amplitude-modulation effect[13] in the dHvA amplitude and as the low-frequency oscillation of approximately 48 T. Branch μ arises from magnetic breakdown because it is only observed at high magnetic fields and over a small angular range about the $\vec{c}$ axis. It is assigned to the ϵ-α orbit. The β orbit is probably also a combination orbit but cannot be assigned unambiguously at the present time.

Thus, the Fermi surface of the incommensurate mercury-chain compound consists of cylinders with axes parallel to $\vec{c}$. They are formed from one-dimensional Fermi-surface sheets normal to $\vec{a}$ and $\vec{b}$ directions by a small interaction of $\vec{a}$ and $\vec{b}$ chains and by translation by a superlattice vector resulting from the incommensurate mercury chains. The electron velocity, being perpendicular to the Fermi surface, is along $\vec{a}$ and $\vec{b}$ directions, giving the high conductivity in the (001) plane that is observed. At this time the magnitude of the superlattice energy gaps is not known and requires further study.

We wish to thank A. J. Berlinsky for useful suggestions regarding the Fermi-surface model and E. Batalla for useful discussions. The research was supported by research grants from the National Research Council of Canada.

[1]B. D. Cutforth, W. R. Datars, A. van Schyndel, and R. J. Gillespie, Solid State Commun. 21, 377 (1977).
[2]C. K. Chiang, R. Spal, A. Denenstein, A. J. Heeger, N. D. Miro, and A. G. MacDiarmid, Solid State Commun. 22, 293 (1977).
[3]E. S. Koteles, W. R. Datars, B. D. Cutforth, and R. J. Gillespie, Solid State Commun. 20, 1129 (1976).
[4]D. L. Peebles, C. K. Chiang, M. J. Cohen, A. J. Heeger, N. D. Miro, and A. G. MacDiarmid, Phys. Rev. B 15, 4607 (1977).
[5]I. D. Brown, B. D. Cutforth, C. G. Davies, R. J. Gillespie, P. R. Ireland, and J. E. Vekris, Can. J. Chem. 52, 791 (1974). This x-ray diffraction meas-

urement gave $3-\delta=2.86$ at room temperature.

[6]R. W. Stark and L. K. Windmiller, Cryogenics 8, 272 (1968).

[7]A. J. Berlinsky, private communication.

[8]J. P. Pouget, G. Shirane, J. M. Hastings, A. J. Heegar, N. D. Miro, and A. G. MacDiarmid, Phys. Rev. B 18, 3645 (1978). We use the low-temperature value, $3-\delta=2.79$, measured by neutron diffraction.

[9]J. E. Graeber and J. A. Marcus, Phys. Rev. 175, 659 (1968).

[10]J. E. Graebner, Solid State Commun. 21, 253 (1977).

[11]L. M. Falicov and M. J. Zuckerman, Phys. Rev. 160, 372 (1967).

[12]J. A. Wilson, Phys. Rev. B 15, 5748 (1977).

[13]M. Alles, and D. H. Lowndes, Phys. Rev. B 8, 5462 (1973).